CAIT-UTC-029

Numerical Simulation of Intelligent Compaction Technology for Construction Quality Control

Final Report
December 2014

Cesar Carrasco
Professor and Department Chair of Civil Engineering
University of Texas at El Paso (UTEP)
El Paso TX 79968

Cesar Tirado
Postdoctoral Research Associate
University of Texas at El Paso (UTEP)
El Paso TX 79968

Hao Wang
Assistant Professor
Rutgers, The State University of New Jersey
Piscataway NJ 08854

External Project Manager
Jimmy Si
Texas Department of Transportation

In cooperation with
Rutgers, The State University of New Jersey
And
State of Texas
Department of Transportation
And
U.S. Department of Transportation
Federal Highway Administration

Disclaimer Statement

TECHNICAL REPORT STANDARD TITLE PAGE

1. Report No.	2. Government Accession No.	3. Recipient's Catalog No.
CAIT-UTC-029		

4. Title and Subtitle	5. Report Date
Numerical Simulation of Intelligent Compaction Technology for Construction Quality Control	December 2014
	6. Performing Organization Code CAIT/UTEP

7. Author(s)	8. Performing Organization Report No.
Cesar Carrasco, Cesar Terado, Hao Wang	CAIT-UTC-029

9. Performing Organization, Name and Address	10. Work Unit No.
The University of Texas at El Paso 500 W University Ave, El Paso, TX 79902	11. Contract or Grant No. DTRT12-G-UTC16

12. Sponsoring Agency Name and Address	13. Type of Report and Period Covered
Center for Advanced Infrastructure and Transportation Rutgers, The State University of New Jersey 100 Brett Road Piscataway, NJ 08854	Final Report 3/01/13 - 12/1/2014
	14. Sponsoring Agency Code

15. Supplementary Notes

U.S Department of Transportation/Research and Innovative Technology Administration
1200 New Jersey Avenue, SE
Washington, DC 20590-0001

16. Abstract

Intelligent compaction (IC) technique is a fast-developing technology for compaction quality control and acceptance. Proof rolling using the intelligent compaction rollers after completing compaction can effectively identify the weak spots and significantly improve the uniformity of the compacted layers. Despite many federal and state funded studies to implement the IC technology, there are still obstacles and gaps that need to be explored and overcome in order to fully employ this technology in the day-to-day operations. What is fundamentally missing from most efforts is an attempt to understand the behavior of the IC roller responses and their correlations to the other modulus-based devices, such as the light-weight deflectometer (LWD). To better understand the process of accepting compacted materials to ensure quality, performance and durability using IC technology, a finite element model was developed to document and understand the theoretical limitations and sensitivity of this technology in order to develop more rigorous specifications. The influence depth for both IC and LWD was studied as well as the level of sensitivity of the stiffness or modulus as measured by these instruments. The nonlinear constitutive model parameters seem to have significant influence on the measured influence depth.

17. Key Words	18 Distributional Statement
Intelligent compaction, MEDPG nonlinear model, Unbound granular base and subgrade material, Lightweight deflectometer, Soil stiffness	

19. Security Classification	20. Security Classification (of this page)	21. No. of Pages	22. Price
Unclassified	Unclassified	30	

Form DOT F 1700.7 (8-09)

Acknowledgments

The authors would like to thank U.S. Department of Transportation and Federal Highway Administration for their financial support, and to thank Rutgers, The State University of New Jersey and Dr. Soheil Nazarian from The University of Texas at El Paso for their coordination.

Table of Contents

List of Figures

List of Tables

1. Introduction

Compaction is an important process in roadway construction necessary to attain high quality and uniformity of pavement materials to better ensure long-lasting performance. Intelligent Compaction (IC) refers to the compaction of pavement materials using vibratory rollers equipped with an integrated measurement system, an onboard computer reporting system, Global Positioning System (GPS) based mapping, and optional feedback control. This new technology provides real-time compaction monitoring and allows for adjustments to the compaction process by integrating measurement and control systems. IC rollers maintain a continuous record of measurements of compaction using Intelligent Compaction Measurement Value (ICMV) which represents the "stiffness" of the materials based on the vibration of the roller drums and the resulting response from the underlying materials. Measurement values are represented as color-coded plots that allow the user to view plots of the location of the roller, the number of passes and stiffness measurements. Yet, measurement values differ considerably among roller manufacturers, as they make use of different methods for calculating these MVs that they claim are associated to the pavement material stiffness.

Pavement structures typically consist of several layers that they progressively become stiffer and thinner as they are constructed. The depth of influence of a roller, which varies with the weight and dimensions of the roller and the amplitude and frequency of the vibration as well as the roller's speed, can be as deep as 1.8 to 2.1 m (6 to 7 ft.) (Mooney et al. 2010). It is intuitive that the thinner the layer that is being compacted becomes, the less influence it will have on the response of the roller. Due to the inevitable variability in moisture content and non-uniformity in soil stiffness of the materials during compaction, there is a minimum layer thickness and modulus contrast that lend the IC roller response ineffective. What complicates the matter more are the facts that geomaterials, such as embankment or base materials, behave quite nonlinearly under the heavy loads of the roller. Understanding the behavior of rollers benefits both contractors and the state highway agencies. The contractor can utilize the results to optimize the roller setting to achieve compaction in the fewest possible passes (an incentive to adopt the technology); while state highway agencies will benefit by minimizing the variability in the IC roller measurements (and as such more confidence in the acceptance results).

The primary tool for quality management of earthwork is currently the nuclear density gauge to ensure that appropriate density is achieved. The density, even though quite practical to measure, is not a parameter that directly ties with the mechanistic-empirical design processes where parameters such as stiffness or modulus are employed. Light Weight Deflectometer (LWD) is an emerging device for evaluating the quality of compacted layers currently accepted by state highway agencies. Relationships between intelligent compaction measurement values (ICMVs) and various in-situ point measurement techniques, such as the LWD, for monitoring compaction of non-granular and granular materials are necessary for quality assurance/quality control (QA/QC) operations and testing.

A large number of case studies of using the IC roller responses side-by-side with other modulus-based methods (e.g., LWD, plate load test, Geogauge, dynamic cone penetrometer, etc.) for acceptance are available in the literature. The results of these studies are mixed primarily because of lack of consideration of roller-soil interaction. Numerical modeling of compact rollers has been previously carried by other researchers. A 2-D finite element (FE) modeling

approach was attempted by Mooney and Facas (2013), though this approach would consider a uniform distribution of responses along the length of the drum. Other researchers considered the unbound granular and subgrade materials to be linear elastic (Patrick and Werkmeister, 2010; Xia and Pan, 2010; Mooney and Facas, 2013) , and some have included the Drucker Prager/cap model (Chiroux et al. 2005; Kim, 2010). Hügel et al. (2008) and Wang et al. (2007) further modeled soil using viscoplastic models. Yet, the nonlinear constitutive model for unbound granular base and subgrade materials as recommended by the MEPDG has not been implemented. In this report, the numerical modeling of a compact roller and a light weight deflectometer on one-layered system consisting of subgrade material modeled using the MEPDG constitutive model is presented in this report. The influence depth was numerically assessed. Though the weight and the roller parameters like amplitude and frequency of vibration may also significantly impact the responses of the rollers, due to time limitation, it is not addressed in this report.

2. Finite Element Modeling of Roller Compaction

The numerical modeling of soil response due to roller compaction is rather complex. Thus, a dynamic finite element technique is necessary to evaluate the dynamic interaction of the roller with the soil or pavement system. For the purpose of this study, a finite element analysis program called LS-DYNA was selected to address this need. LS-DYNA is a multi-purpose FE program that makes use of explicit and implicit time integration techniques. A 3-D mesh was built for the FE modeling of a roller compacting the soil with a vibrating frequency. Figure 1 shows a 3-D view of the pavement structure and the roller. As shown in the figure, the drum was modeled with rigid shell elements and dimensions typical to common IC rollers: 2 m (80 in.) wide and 0.75 m (30 in.) in radius. Due to the size of drum, the soil was modeled 4 m (160 in.) wide, 4 m (160 in.) in length, and 2.5 m (100 in.) in depth. A mesh consisting of brick elements was used for the pavement structure. Smaller elements with 50×50×50 mm (2×2×2 in.) dimensions were used underneath the roller up to 0.5 m in depth, 0.6 m longitudinally and 1.2 transversally from the center of the roller, after which they become larger in size. A total of 63,840 elements were used in the soil. The roller was positioned at the center of the model. 75,360 shell elements were used to define the roller to better accommodate its nodes to be in contact with the soil's mesh. The interaction between the roller and the pavement structures was modeled using the automatic single surface contact option of LS-DYNA. Figure 2 shows the roller to surface contact.

The vibratory loading of the roller was modeled using a 30 Hz sinusoidal load distributed on the roller, with an amplitude of 350 kN (78.7 kips), in addition to the 6000 kg mass (13 kips) corresponding to the roller. In addition to the geometric damping that occurs naturally in the model, Rayleigh damping was introduced to simulate material damping in the soil. The damping matrix [C] is defined by two parameters α and β as defined in Equation 1.

$$[C] = \alpha[M] + \beta[K] \tag{1}$$

where [M] is the mass matrix, [K] is the stiffness matrix, α and β were arbitrarily defined as 25 and 0.0002.

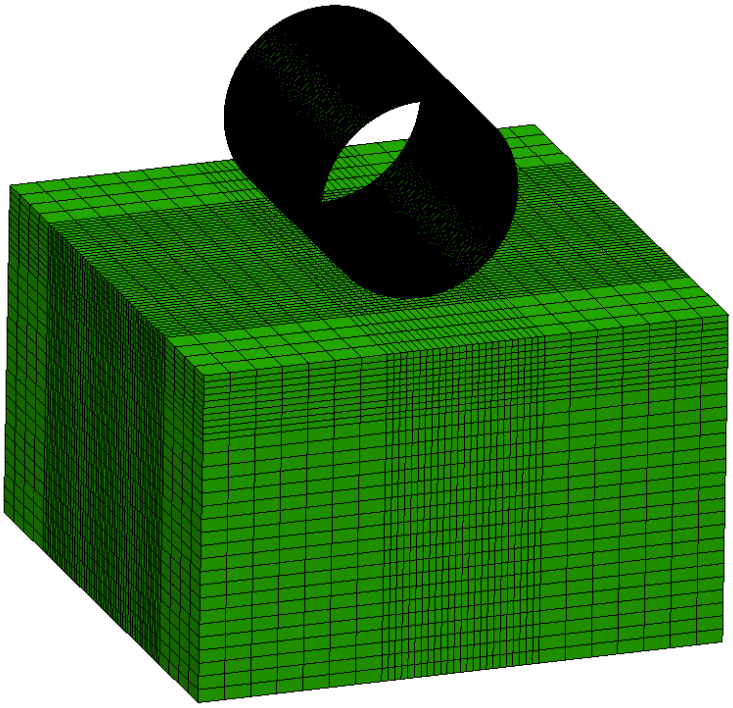

Figure 1 - FE modeling of roller and pavement structure

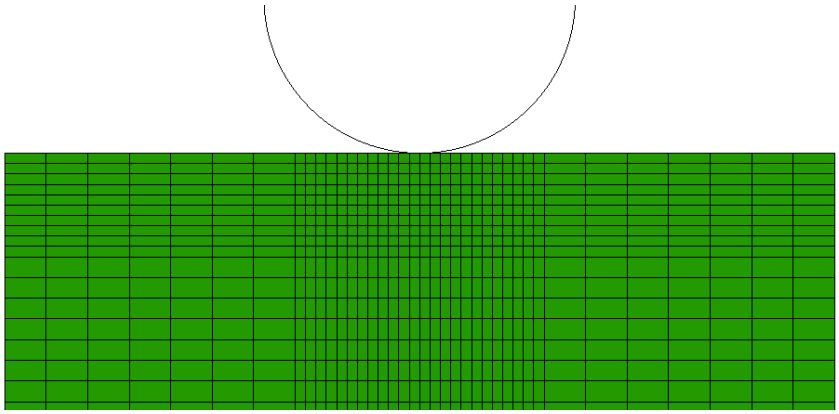

Figure 2 – Roller to soil contact

2.1 Characterization of Unbound Granular Bases and Subgrades

Most highway agencies use the MEPDG-recommended constitutive model to determine the resilient modulus M_R used to predict the nonlinear behavior of unbound granular materials:

$$M_R = k_1 P_a \left(\frac{\theta}{P_a} \right)^{k_2} \left(\frac{\tau_{oct}}{P_a} + 1 \right)^{k_3}, \quad (1)$$

where P_a is the normalizing stress, i.e. atmospheric pressure of 101.4 kPa (14.7 psi), θ is the bulk stress, τ_{oct} is the octahedral shear stress, and k_1, k_2, k_3 are regression coefficients determined from laboratory testing. MEPDG uses a hierarchical approach for the design inputs based on the project importance and available resources. Three levels of inputs are provided for characterization of resilient properties of unbound materials. MEPDG recommends the

measurement of resilient modulus parameters from the laboratory testing (Level 1), through the use of correlations with other material properties (Level 2) or estimating them on the basis of soil classification (Level 3). The input level selected affects the procedure for determining the structural responses of the pavement system (Khazanovich et al. 2006).

The moduli required for design purposes must represent the state of stress due to vehicular loads and overburden pressure. Since the state of stress in pavements is a function of the selected moduli, a rigorous process for selecting the modulus has to be through an iterative process. To simplify this process, NCHRP 1-28A recommended the states of stress of θ = 213.7 kPa (31 psi) and τ_{oct} = 51.7 kPa (7.5 psi) for base and subbase materials, and θ = 85.5 kPa (12.4 psi) and τ_{oct} = 20.7 kPa (3 psi) for subgrade soils (Oh, 2011).

2.2 Parametric Study

A parametric study was carried out on a one-layer system. Parameters were selected for each of the typical range of k' values for fine-grained materials appropriate for the nonlinear constitutive model, as shown in Table 1. The values shown in Table 1 were selected within the feasible ranges of nonlinear k parameters proposed from (Velasquez et al. 2009) for fine-grained materials: k_1 = 1,000 to 6,000; k_2 = 0.01 to 0.5; k_3 = -6.0 to -1.5.

The vibratory motion of the roller was kept until t = 200 ms, completing six load application cycles. Pressure and displacement contours were generated for every time interval of 1 ms during the analysis. Time history pavement responses were measured underneath the center of the roller. With this information, profiles of vertical deflection, stress and strain were measured during the roller impact to calculate the depth of influence of loading has on the pavement structure.

Table 1. Pavement Sections Properties for One-Layered System

Pavement Properties	Value
k'_1	400, 1500, 3000
k'_2	0.01, 0.20, 0.40, 0.80
k'_3	0.0, -1.0, -2.0, -3.0, -4.0
Poisson's ratio, ν	0.35

2.3 Investigating Influence Depth

The vertical stress profiles with respect to depth for a geomaterial with k_1=1500, k_3=0 and varying k_2 are shown in Figure 3a. These profiles are obtained from the first cyclic peak responses. Stresses vary from 0.87 MPa (125 psi) to 1.27 MPa (185 psi) on the surface, all decreasing to about 0.20 MPa (29 psi) at 0.50 m below the soil surface. Figure 3b shows the depth profile for vertical stress normalized with respect to the peak stress, occurring at the surface. From this figure it can be seen that a load influence based on a 10% stress of the surface stress occurs at about 1.0 m below the surface.

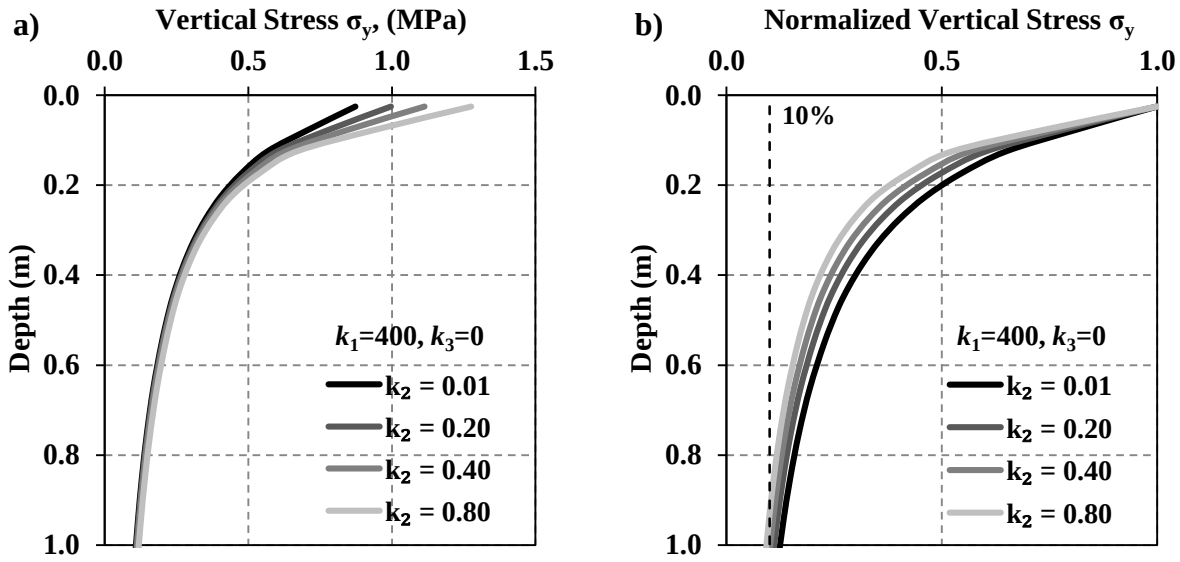

Figure 3 – Depth profiles for vertical component of (a) stress and (b) stress normalized with respect to surface stress under roller compaction for soils with k_1=400, k_3=0, and varying k_3.

Likewise, Figure 4a shows the deflection profile with respect to depth for the same geomaterials. Deflection at the surface varied greatly depending the magnitude of k_2. Figure 4b shows the depth profile for vertical deformation normalized with respect to the surface deflection. Unlike the stress responses, the load influence based in terms of deflection based on a 10% surface deflection criterion occurs at about 2.0 m below the surface.

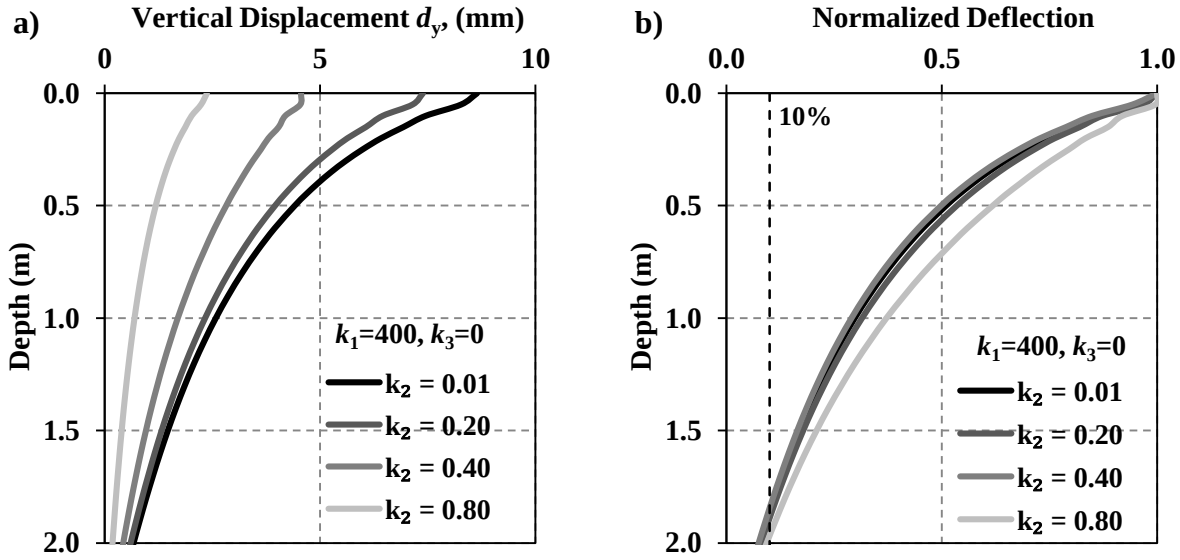

Figure 4 – Depth profiles for of (a) deflection and (b) deflection normalized with respect to surface deflection under roller compaction for soils with k'_1=400, k'_3=0, and varying k'_3.

Depth of influence of soil compaction was calculated using the cyclic peak responses in terms of stress, strain and deflection for different material properties using the procedure shown on the normalized responses from Figures 3 and 4. Mooney et al. (2010) suggested measurement depths of about 1.2 m (47 in.). Measurement depth, H_c, is reached when the pavement response (stress, strain, deflection) decayed to about 10% of surface (peak) response value.

Figure 5 shows the depth of influence in terms of stress at 10% of the surface stress. Influence depth decreases slightly with stiffer materials (i.e. higher k_1) and for more granular materials (i.e. higher k_2) as shown in Figure 5a. However, k_3 has a significant impact on influence depth, as shown in Figure 5b, as the depth of influence significantly increases with more clayey materials.

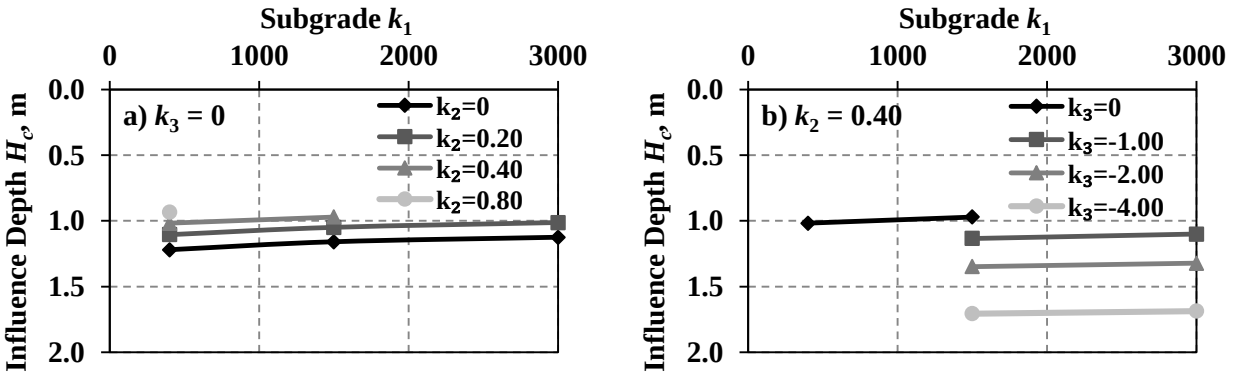

Figure 5 – Influence depth based on vertical stress at 10% of surface stress for varying k_1 and k_2, and k_3=0, and (b) varying k_1 and k_3, and k_2=0.40

Likewise, the depth of influence in terms of deflection was evaluated. Figure 6a shows the influence depth for different k_1 and k_2 values, maintaining a k_3 constant. From such figure it can be seen no significant change in influence depth with stiffer or more granular materials as long as k_3 remains constant. Yet, when the material becomes more clayey, the depth of influences varies considerably as shown in Figure 5b. It must be pointed out that cases where the state of stress under the roller caused the resilient modulus, as calculated per the MEPDG nonlinear constitutive model, to drastically fell outside the reasonable ranges of subgrade moduli were excluded.

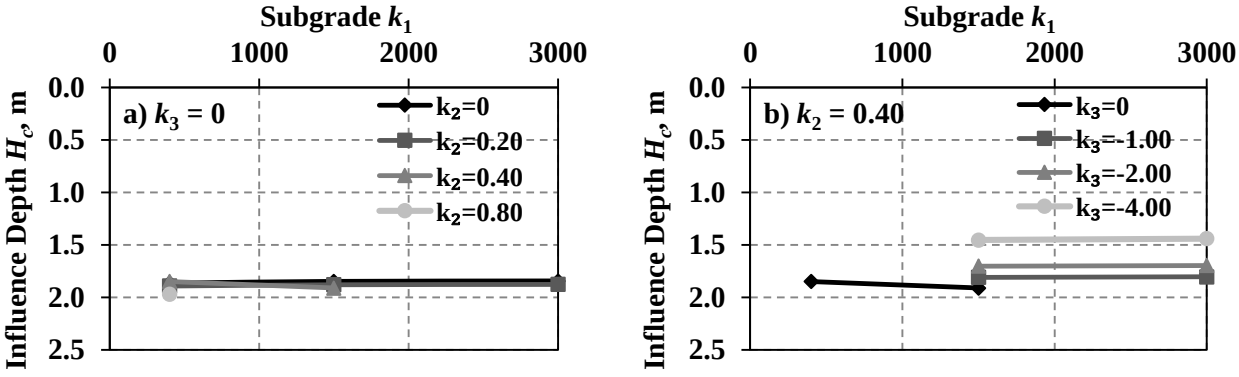

Figure 6 – Influence depth based on vertical stress at 10% of surface stress for varying k_1 and k_2, and k_3=0, and (b) varying k_1 and k_3, and k_2=0.40

Both Figures 5 and 6 indicate that influence depth based in terms of stress and deflection is highly dependent on the k_3 parameter (telling how clayey is the material), and both can reach up to 2 m in depth.

It was not possible to predict the influence depth at 10% of peak surface vertical strain for all cases, since some cases extended beyond the model's depth of 2.5 m. Depth of influence at 10% of the selected surface peak response level usually occurs at a point where the slope created from the response vs. depth plot is approaching verticality, particularly for stress and strain, as shown in Figure 3.

2.4 Evaluating Stiffness

Two soil stiffness parameters are used in current practice. These parameters are determined from cyclic drum deformation. Thus, force-displacement hysteresis loops are developed by plotting the time-varying contact force F_c versus drum displacement z_d (Mooney et al. 2010). In the case of the numerical analysis, the vertical force transferred to the soil surface and the vertical deformation of the soil surface is used. Figure 7a shows a sample hysteresis loop for a pavement with a 6-in. base, 45 ksi base modulus and 15 ksi subgrade modulus whose responses were obtained after a linear elastic analysis. This pavement is included as it better explains how the stiffness can be determined. Downward direction is taken as positive for both force and displacement. The secant stiffness k_s is calculated from the point of zero dynamic displacement (under static loading) to the point of maximum displacement. This parameter is used by Case/Ammann as a measurement value after roller compaction (Rinehart and Mooney, 2009). The tangent stiffness k_t is measured from the loading portion of the curve as used by Bomag for determining E_{vib}.

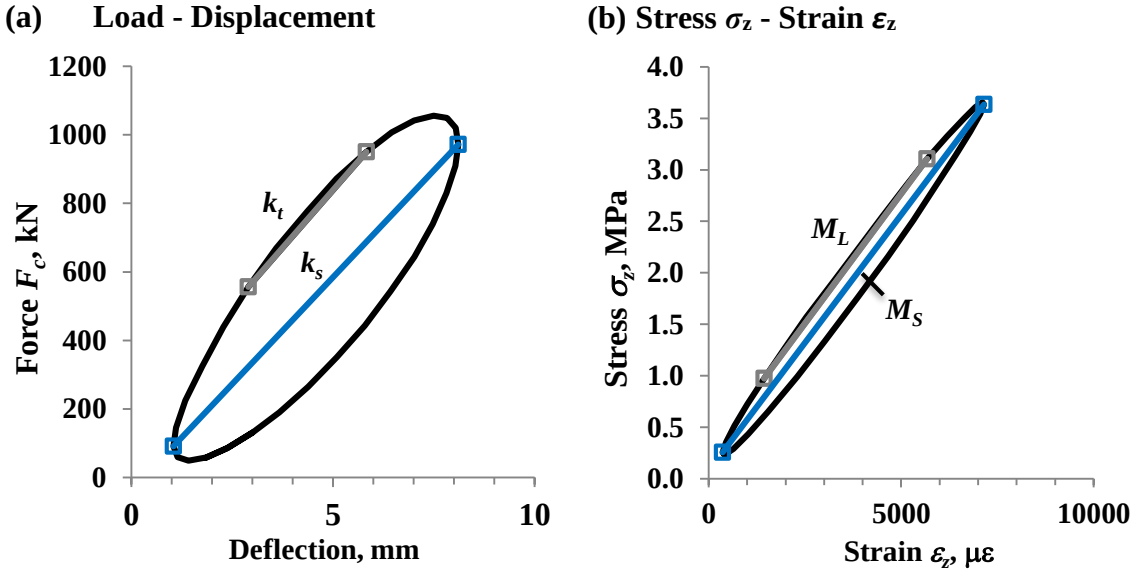

Figure 7 – Determination of tangent and secant (a) stiffness and (b) modulus from hysteresis loops for a 6-in. base, E_{BASE} = 45 ksi and E_{SUBG} = 15 ksi, linear elastic FE analysis.

Similar to the process for determining stiffness from hysteresis, tangent and secant modulus can be obtained from the stress-strain σ_z-ε_z hysteresis loops. Figure 7b shows the σ_z-ε_z response to a vibratory roller pass. Secant modulus M_S is determined from zero σ_z-ε_z or the point of minimum through maximum ε_z. Tangent modulus M_L is calculated similar to tangent stiffness. Figure 7b shows a hysteresis σ_z-ε_z loop for the same pavement modeled linearly elastic. Compressive stress and strain are taken as positive.

Load-deflection and stress-strain hysteresis curves depicting 6 vibration cycles for a subgrade material with k_1 = 400, k_2 = 0.40 and k_3 = 0 properties are shown in Figures 8a and 8b, respectively. Flattening observed in the load-displacement hysteresis curve close to the end of the cycle occurs due to the loss of contact of the roller to the ground.

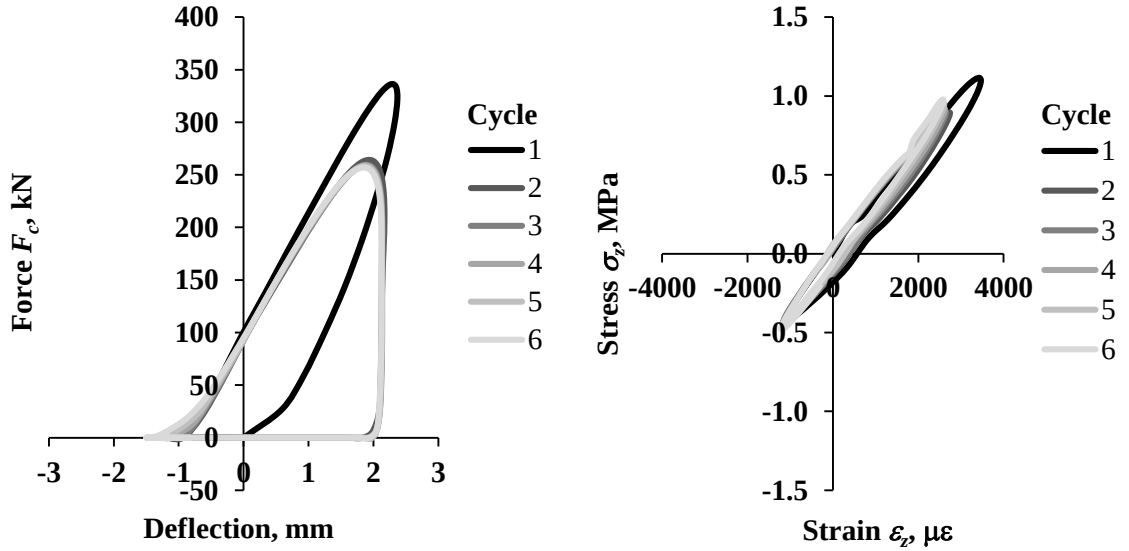

Figure 8 –Hysteresis loops based on (a) load-deflection and (b) stress-strain for a geomaterial with parameters k_1 = 400, k_2 = 0.40 and k_3 = 0 properties as per the MEPDG nonlinear constitutive model.

Little variation is observed in stiffness and modulus after each cycle in the material shown in Figure 8, which has some level of granularity (k_2 = 0.40); however, when the material becomes more clayey (higher k_3) both mechanical properties (stiffness and modulus) exhibit a significant change in the magnitude of these properties after every cycle. In this report, only the study of the response to the first cycle will be presented.

Figure 9 shows tangent stiffness, k_t, and tangent modulus, M_L, for different geomaterials with varying k_1 and k_2 nonlinear parameters, and k_3 = 0, as obtained from their respective soil surface hysteresis loops. From such figure, it can be seen that both properties increase when the material becomes stiffer (k_1) and more granular (k_2). Yet, depending on the magnitudes of k_1 and k_2, the material stiffness and modulus can yield extremely high magnitudes outside the typical ranges of a subgrade material. For instance, modulus can reach up to 840 MPa (120 ksi) when k_1 = 3000, k_2 = 0.20 and k_3 = 0 (see Figure 8b), a magnitude even large for a granular base material. These magnitudes are observed as the MEPDG model yields high resilient modulus values due to the

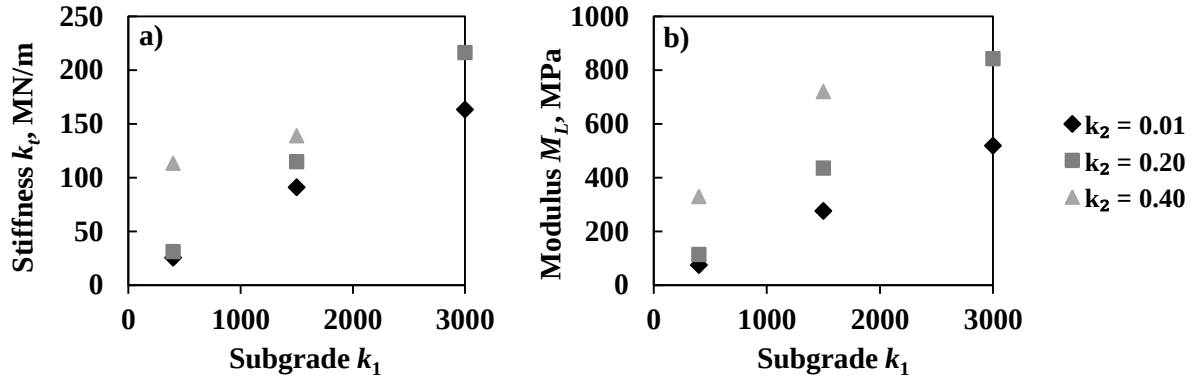

Figure 9 – (a) Tangent stiffness and (b) tangent modulus for different geomaterials with varying k_1 and k_2, and k_3 = 0.

large stresses occurring underneath the roller at the soil surface at peak loads. In the aforementioned pavement case, bulk stress, θ, reaches 1.10 MPa (320 psi.) at the soil surface at peak load. Setting limits to the constitutive model may be recommended but may cause instability during the finite element analysis.

Figure 10 shows tangent stiffness, k_t, and tangent modulus, M_L, for different geomaterials with varying k_1 and k_3 nonlinear parameters, and k_2 = 0.40, as obtained from their respective soil surface hysteresis loops. From this figure, both mechanical properties decrease with higher k_3, i.e. as the material becomes more clayey. Again, depending on the magnitude of the nonlinear parameters, the geomaterials mechanical properties may fall outside the typical ranges proper to a subgrade material.

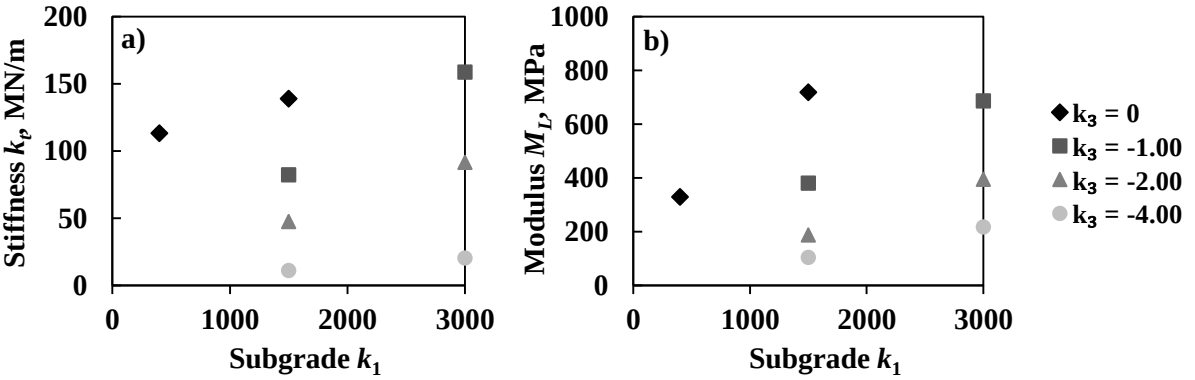

Figure 10 – (a) Tangent stiffness and (b) tangent modulus for different geomaterials with varying k_1 and k_2, and k_2 = 1.50.

Figure 11a shows tangent and secant stiffness with respect to the resilient modulus of the geomaterial as calculated using the recommended MEPDG representative stresses for subgrade materials, i.e. 85.5 kPa (12.4 psi) and τ_{oct} = 20.7 kPa (3 psi), as proposed by Oh (2011) after a study carried in NCHRP 1-28A. Similarly, Figure 11b shows tangent and secant modulus with respect to the MEPDG representative resilient modulus. In the latter figure it can be seen that the proposed representative state of stress significantly underpredicts the soil response when compared to the nonlinear response.

(a) Stiffness

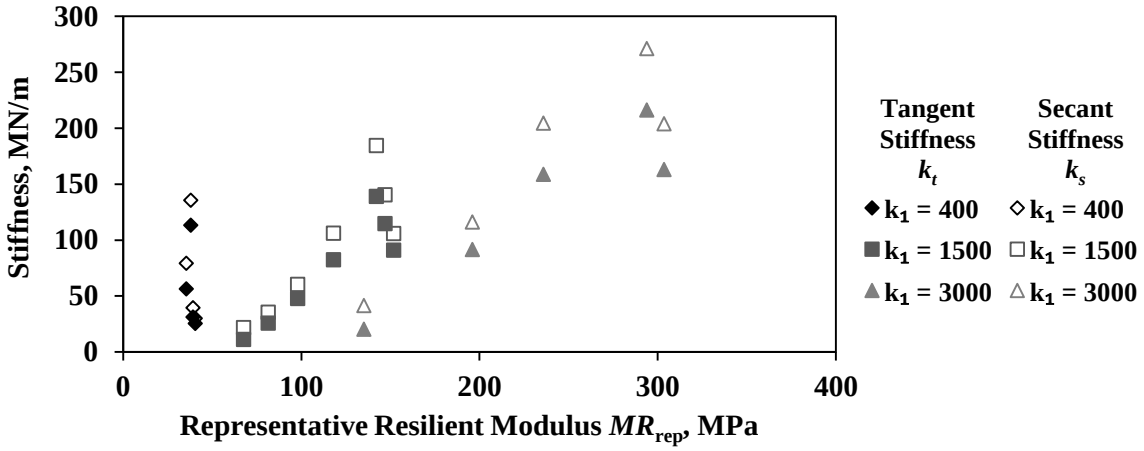

(b) Modulus

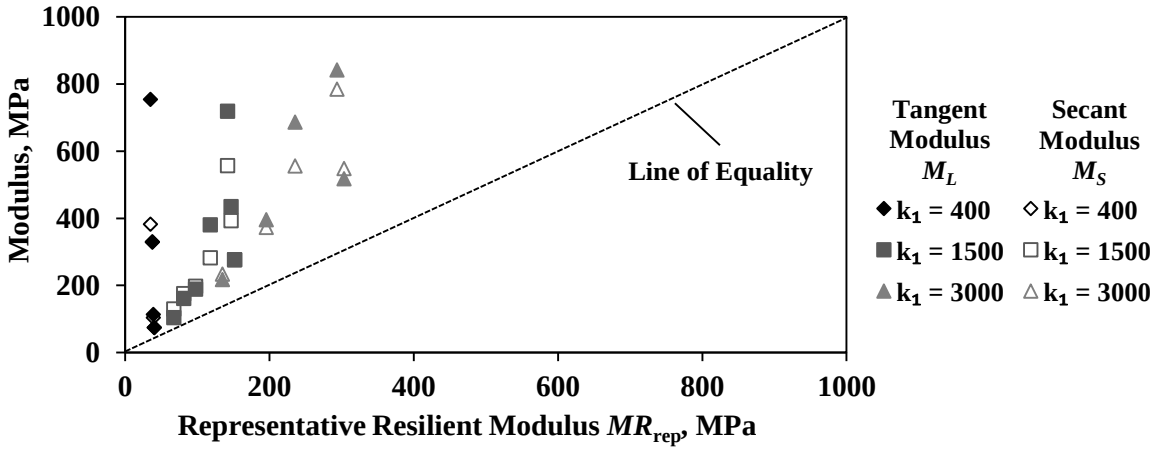

Figure 11 – Secant (a) stiffness and (b) modulus for both 6 and 12 in. base thickness with respect to base to subgrade modulus ratio.

3. Numerical Modeling of Light Weight Deflectometer (LWD)

The implementation of the new mechanistic-empirical design guide (MEPDG) requires the modulus parameters of each unbound pavement layer. The current state of practice in construction quality control is based on a density and sometimes restricting the moisture variations. A stiffness-based approach would be favorable to accommodate for the missing link between design and quality control processes. Among the several devices developed to address this gap, the Light Weight Deflectometer (LWD) is gaining popularity upon success of its predecessor, i.e., the Falling Weight Deflectometer (FWD). LWD is one the QC/QA nondestructive devices that is gaining popularity due to its portability and simplicity of deflection-based concept during the implementation of mechanistic empirical methods. Several studies have been dedicated to evaluation of LWD device and the dependency of the results on many of the device specifications. The estimated deflection, which is transformed to modulus assuming a half space elastic layer theory, is affected not only by the stiffness of the top layer, but also the properties of the underlying layers. As such, determining the influence depth of the device is an important part of the quality acceptance plan based on the LWD results.

During LWD tests, the response of a pavement layer to the impact load is measured. The response largely depends on the falling mass, typically of 10 kg (22 lb), though it can go up to 20 kg (44 lb); plate diameter, typically from 150 mm (6 in.) to 300 mm (12 in.); the drop height; the LWD buffer stiffness and the properties of the underlying layers. Therefore, different types of LWD devices may yield different responses on the same type of geomaterial. The duration of the LWD impulse load is usually between 15 msec to 30 msec. Some types of LWD devices measure the deflection of the plate while assuming a constant impulse load (e.g., Zorn® LWDs). Others estimate the deflection of the soil at the plate-soil interface through a displacement sensor (geophone) (e.g., Dynatest LWD). Nevertheless, the LWD modulus is calculated based on the same Boussinesq assumptions of an elastic half-space. Several studies have evaluated the factors influencing the LWD modulus through extensive laboratory and field experiments (Fleming et al. 2000; Alshibli et al. 2005; White et al. 2009). Some others developed analytical methods to evaluate the response of the pavement layers under the LWD impact (Stamp and Mooney, 2013; Bilodeau and Doré, 2014).

Fleming et al. (2000) and Siekmeier et al. (2000) reported the influence depth of the LWD about the same as the diameter of the loading plate. Nazzal et al. (2004) reported the depth of influence of the LWD between 1.2 and 1.4 times the plate diameter. Mooney and Miller (2009) employed a stress-strain measurement approach to investigate the response of three different soil layers under the LWD loading. They buried earth pressure cells and LVDTs at different depth of constructed layered soil systems and tested one type of LWD device with variable load and plate size. Independent of the peak load, the influence depth of about 2 times the plate diameter was measured based on the stress distribution. The depth of influence based on strain measurements varied between 0.5 and 1.1 times the plate diameter.

Similar to the modeling of the IC, a numerical finite element model was developed to investigate the analytical responses of different pavement sections to the two popular types of the LWD devices. The analyzed LWDs were Zorn ZFG 2000, which complies with ASTM E2835, and Dynatest 3031 that complies with ASTM E2583. Although both devices theoretically perform the same tests, they produce different deflections under the same applied load. The differences in the LWD responses are partly attributed to the different load pulse shapes of the LWD devices, differences in deflection transducers and their location, and plate contact stress, among other factors that affect the calculation of surface modulus (Vennapusa and White 2009; Mazari et al. 2014). In this study, stress and strain criteria were employed to determine the measurement depth with each type of the device. The main objective of these analyses is to establish the influence depth of each device with respect to layer properties as well as device configurations. These results will eventually serve for the development of transfer functions for relating the mechanical properties of the soil as obtained by the LWD to the ones as obtained from the IC roller technologies.

3.1 Finite Element Modeling of Light Weight Deflectometer (LWD)

An axisymmetric dynamic nonlinear FE model was developed using LS-DYNA to simulate the light weight deflectometer testing on top of a geomaterial. The Zorn and Dynatest LWDs were modeled differently, as shown in Figure 12. Four-node isoparametric elements were used for both soil and LWD loading plate. A total of 100,000 elements were used for modeling the soil,

with bottom and lateral extent boundaries located 2 m (80 in.) away from the soil-plate contact surface. The 200-mm diameter LWD loading plates were modeled using a linear elastic material rather than rigid. Impact was simulated as a pressure load exerted by the footprint of the housing for the Dynatest and within a 25 mm (1 in.) diameter area corresponding to ball protruding from the top of the Zorn unit. To rule out the differences in responses due to the different impact loadings of those devices, the simulated LWD impact for both devices consisted of a 6.67 kN (1500 lb) force with a pulse duration of 17 msec.

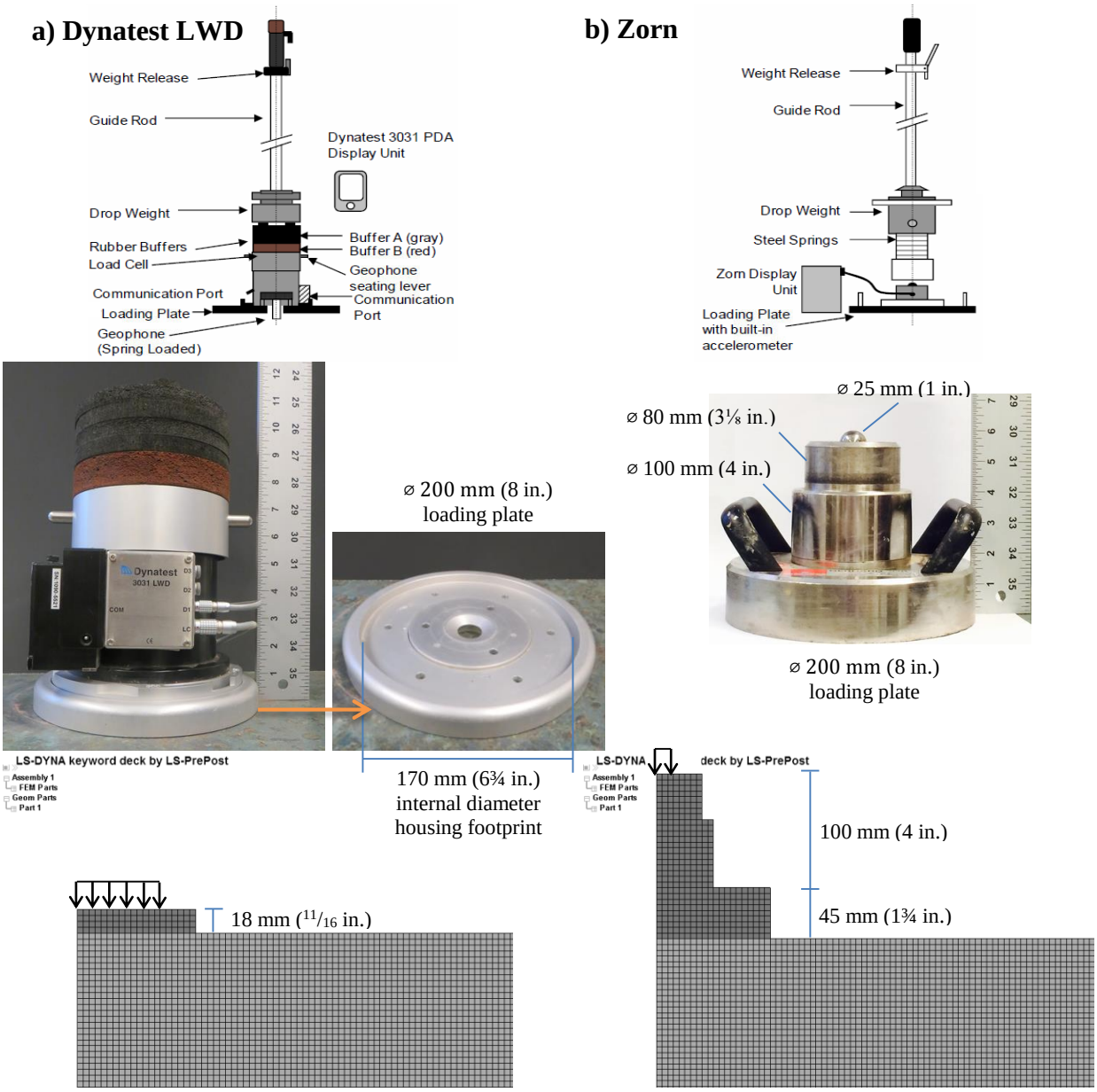

Figure 12 – Schematic views of devices and finite element models for (a) Dynatest LWD and (b) Zorn LWD.

Figure 13 compares the stress distribution of the soil observed in the field under the LWD plate with the uniform stress distribution typically assumed in the analysis. To account for the realistic

stress distribution in the soil due to the soil-plate interaction, a 2-D surface-to-surface contact model was incorporated in the FE model.

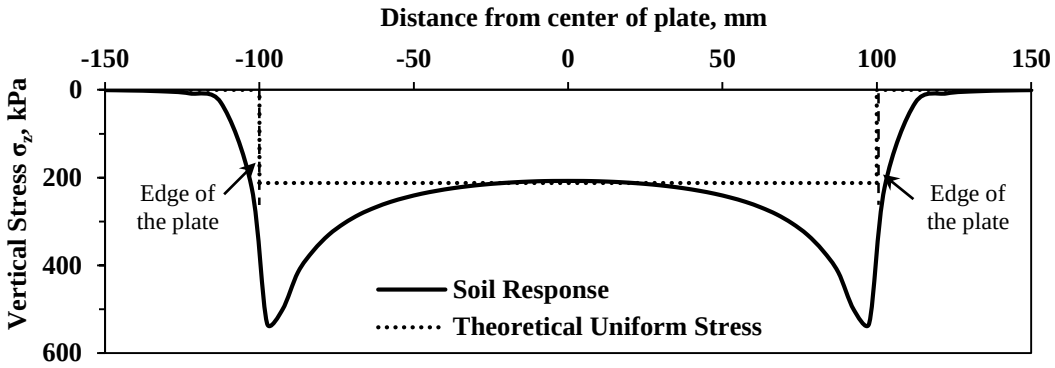

Figure 13 – Soil response under LWD and theoretical uniform stress.

Geomaterials were modeled using a modified nonlinear constitutive model as proposed by Ooi et al. (2006), based on the MEPDG constitutive model for unbound granular and subgrade materials,

$$M_R = k_1' P_a \left[\frac{\theta}{P_a} + 1 \right]^{k_2'} \left[\frac{\tau_{oct}}{P_a} + 1 \right]^{k_3'} \quad (1)$$

where θ = bulk stress, τ_{oct} = octahedral shear stress, P_a = atmospheric pressure, and k'_1, k'_2, and k'_3 are regression coefficients determined from laboratory testing. Mazari et al. (2014) found the modified constitutive model accounts better for the observed differences between the experimental and analytical pavement, and they provide relationships between this model and the MEPDG constitutive model.

To determine the influence depth of the LWDs, a parametric study was carried on a one-layer uniform geomaterial. Table 2 shows the ranges of the nonlinear k' parameters considered in this study.

Table 2. Properties for One-Layer System for Parametric Study of LWD.

Pavement Properties	Value
k'_1	400, 1500, 3000
k'_2	0.01, 1.50, 3.00
k'_3	0.0, -2.0, -4.0
Poisson's ratio, ν	0.35

Time histories of responses were measured underneath the center of the plate and along the soil surface with a 1 kHz sampling frequency. With this information, profiles of vertical stress, strain and deflection were calculated during the plate impact.

3.2 Investigating Influence Depth

Depth of influence of the LWD impact was studied using the selected parameters shown in Table 2. The vertical stress profiles with respect to depth for a geomaterial with k'_1=400, k'_3=0 and varying k'_2 is shown in Figure 14a. The vertical strains and deflections with respect to depth for the same soil types are shown in Figures 14b and 14c, respectively. Unlike for the vertical stresses, the nonlinear parameters clearly have a significant effect on the soil deformation.

Figure 15 shows the depth of influence of the two LWDs defined as the depth where the stress is equal to 10% of the surface stress. The influence depth varies between z/D = 2.0 and 2.5. The depth of influence decreases as the material becomes more granular, i.e. higher k'_2. Likewise, the depth of influence decreases as the material becomes stiffer, i.e. higher k'_1, particularly under Dynatest LWD loading. Parameter k'_3 does not seem to impact significantly the influence depth, as shown in Figure 4b. Moreover, the influence depths of the Zorn LWD are deeper than the Dynatest LWD. This trend could be attributed to the different contact stress profiles occurring at the soil-plate interface caused by the LWD impact of these devices.

Figure 16 shows the variations in vertical stress in soil immediately under the two LWD plates for three geomaterials with varying k'_2 (k'_1 = 400 and k'_3 = 0). Both plates concentrate pressure at the outer edges of the plates while having reduced pressure towards the center of the plates. Despite having the same 6.67 kN (1500 lb) impact load, higher stresses develop under the Zorn plate. This is due to the different stress distributions within the loading plates: The mass drop impacts a surface within a 140-mm (5.5 in.) diameter at the top of the Dynatest LWD loading plate while for the Zorn LWD the impact occurs within a 25-mm (1 in.) diameter area.

Figure 17 shows the vertical stress variations through both LWD plates and the top portion of the soil. Fringe levels, shown in Pascal units, were limited to a magnitude of 500 kPa in compression, cropping higher compression values actually occurring within the darker shaded areas. The stress propagates within Zorn LWD loading plate towards its outer boundary creating a higher stress concentration at the edge of the plate. Also, the Zorn LWD loading plate transfer more energy to the soil than the Dynatest LWD. Vertical stresses under the Zorn LWD are on average 1.5-1.6 times greater than those of the Dynatest LWD. The higher stress concentration on the soil surface under the edge of the two plates then propagates downward towards the center of the plate causing slightly higher stresses at about z/D = 0.5 than those at the surface.

A similar phenomenon occurs with the strain profile, as shown in Figure 14b. Vertical strains significantly increase from the surface reaching a maximum at a depth of 100 mm (z/D = 0.5) then followed by a decrease in compressive strain with respect to depth. Figure 18 shows the vertical strains under the LWD plates. The range of fringe values was set to be identical for the two devices to show higher compressive strains that are developed under the Zorn LWD. Peak vertical strains ($\varepsilon_{z\text{-peak}}$) under the Zorn LWD are usually 1.2 to 1.8 times greater than those under the Dynatest LWD.

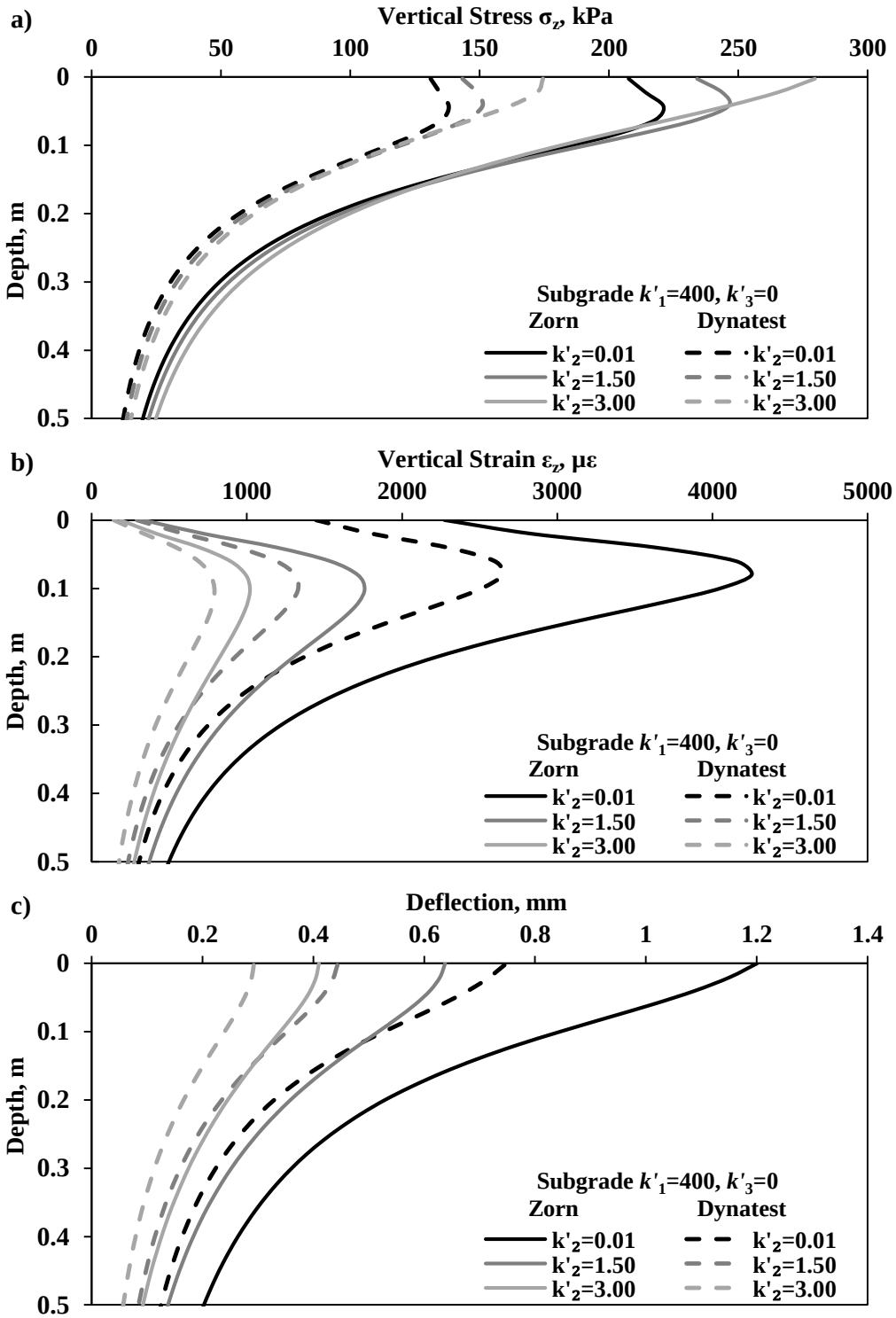

Figure 14 – Depth profiles for (a) vertical stress, (b) vertical strain and (c) deflection under Zorn and Dynatest LWD plates.

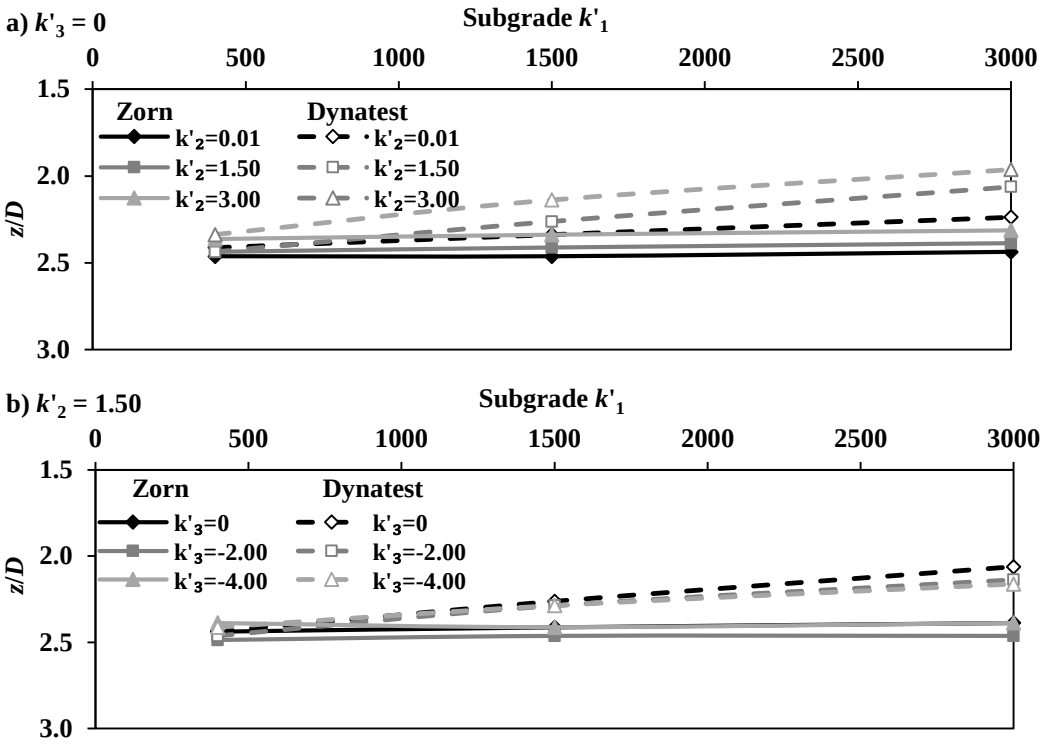

Figure 15 – Influence depth in terms of plate diameter (*z*/*D*) based on vertical stress at 10% of surface stress for both Zorn and Dynatest LWD.

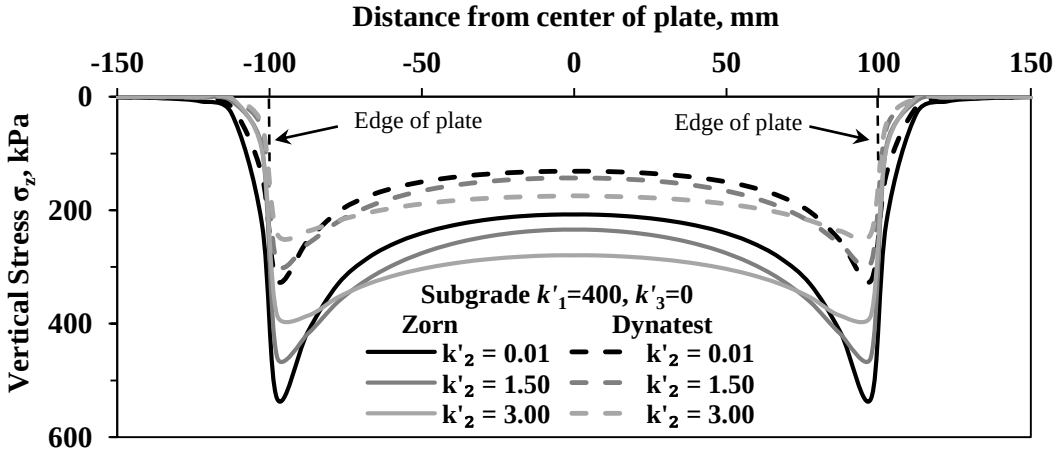

Figure 16 – Stress profiles under Zorn and Dynatest LWD plates for subgrade with varying k'_2, k'_1=400 and k'_3=0.

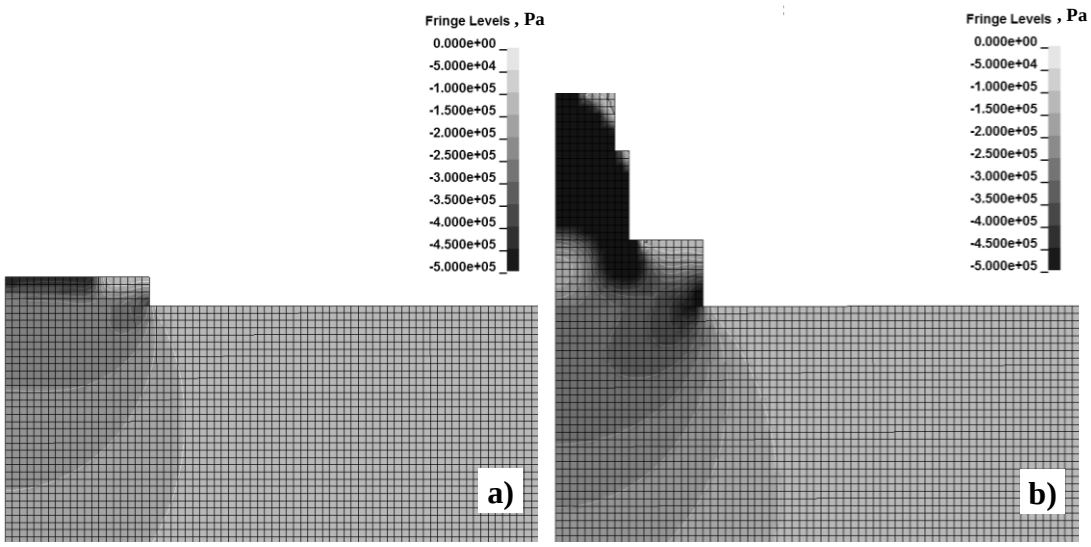

Figure 17 – Stress propagation, vertical component, through geomaterial subjected to (a) Dynatest LWD and (b) Zorn LWD testing.

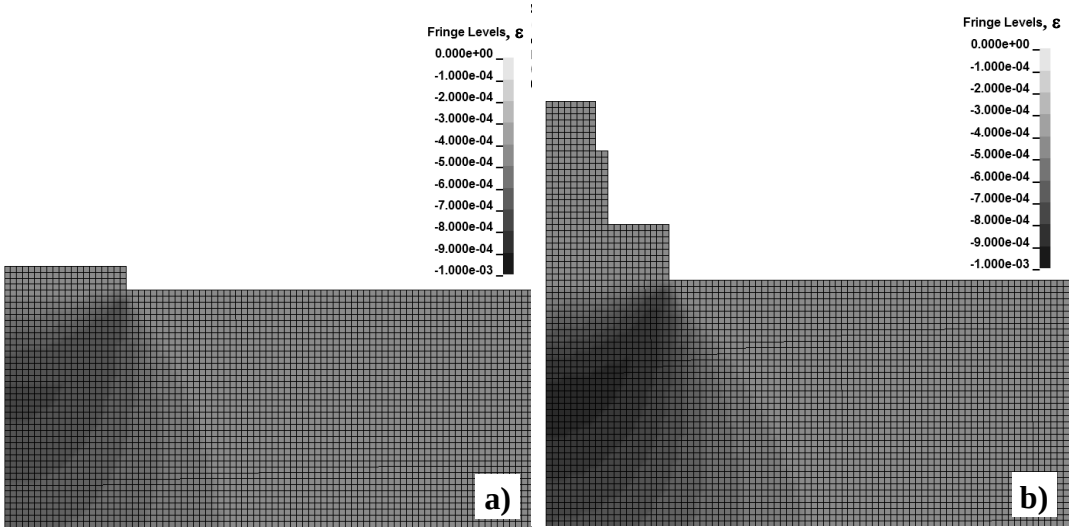

Figure 18 – Strain propagation, vertical component, through geomaterial subjected to (a) Dynatest LWD and (b) Zorn LWD testing.

Figure 19 shows the depth where the strain is equal to 10% of the maximum compressive strain. This depth occurs within a range of $z/D = 2.0$ and $z/D = 3$. These values are greater than what is predicted from other studies because the dynamic nature of the model and the nonlinear behavior of the geomaterials are taken into account.

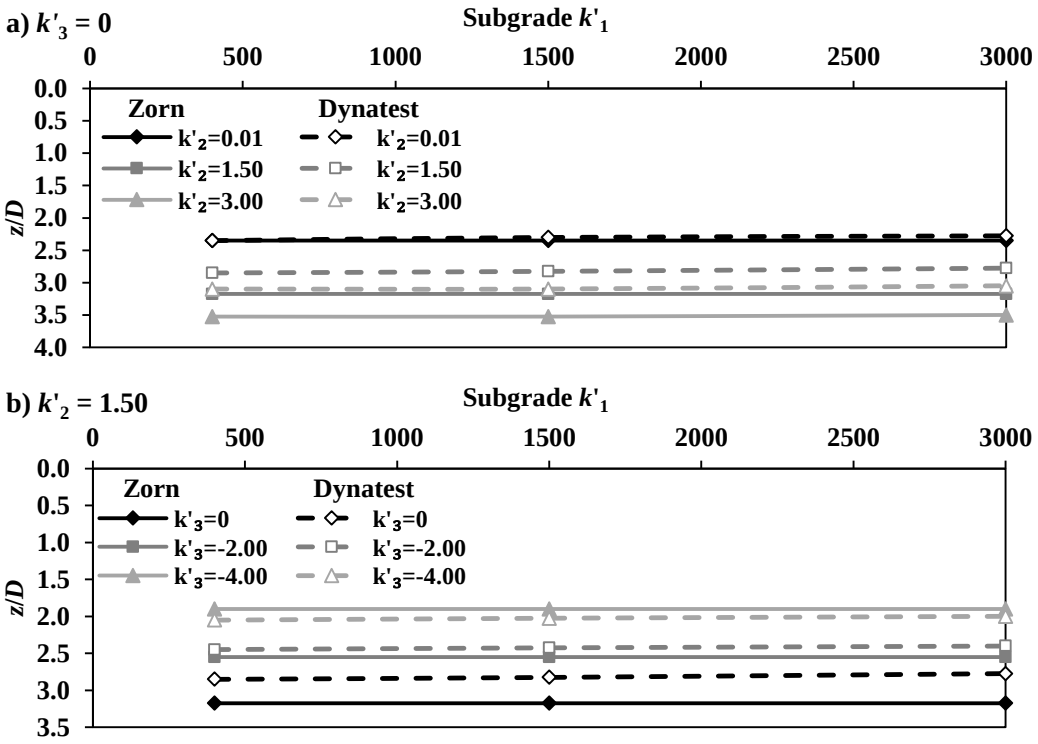

Figure 19 – Influence depth in terms of plate diameter (*z*/*D*) based on vertical strain at 10% of maximum strain for both Zorn and Dynatest LWD.

Depths of influence of the two devices in terms of strain increase when more granular materials is used, i.e., higher k'_2, as shown in Figure 19a, and decreases with more clayey materials, i.e., higher k'_3, as shown in Figure 19b. In this case, stiffness parameter k'_1 does not seem to have a significant impact on the depths of influence. Moreover, lower influence depths are observed for the Dynatest LWD.

Figure 20 shows the depth of influence determined in terms of 10% of surface deflection varies between $z/D = 3$ and $z/D = 4$. The influence depth decreases with lower k'_2, i.e., when material is less granular, as shown in Figure 20a, and with higher k'_3, i.e. more clayey material, as shown in Figure 20b. Yet, influence depth is not sensitive to parameter k'_1 which is the parameter related to stiffness. These trends are similar to those obtained from the strain-based influence depths. Generally, the Zorn LWD demonstrates a slightly greater deflection-based depth of influence as compared to the Dynatest LWD.

Deflection-, strain- and stress-based depths of influence are material and device dependent. The Zorn LWD seems to be less sensitive to the nonlinear soil parameters as compared to the Dynatest LWD.

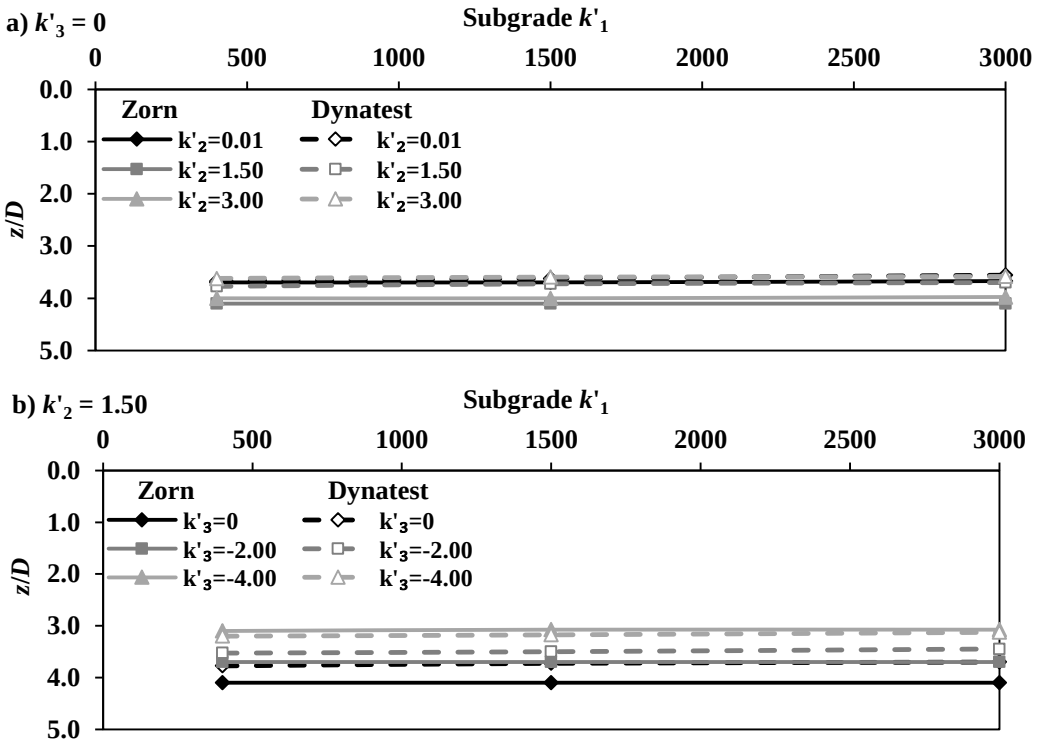

Figure 20 – Influence depth in terms of plate diameter (*z*/*D*) based on deflection at 10% of surface deflection for both Zorn and Dynatest LWD.

3.3 Evaluating Surface Modulus

The surface modulus E_{LWD} is determined using the Boussinesq solution (Terzaghi and Peck 1967):

$$E_{LWD} = \frac{\left(1-\nu^2\right) a\sigma_0}{d_{LWD}} \times f \tag{2}$$

where ν is Poisson's ratio, σ_0 is the uniformly distributed applied stress under the plate, a is the radius of the plate, d_{LWD} is the soil surface deflection at the center of the plate, and shape factor is assumed to be $f = \pi/2$, suiting the inverse parabolic distribution of the soil response. As a result of greater deflections under the Zorn LWD than those under the Dynatest LWD, lower moduli are obtained for the Zorn than the Dynatest LWD (see Figure 21). Using the soil responses for all cases considered, the following relationship is established to relate the Zorn and Dynatest LWDs' surface moduli, E_{LWD}:

$$E_{\mathrm{LWD\ Dynatest}} = 1.65 E_{\mathrm{LWD\ Zorn}} \quad (R^2 = 0.99). \tag{3}$$

A larger database of LWD pavement responses is under development. This database will consist of both single and two-layered systems (base and subgrade) with the purpose relating LWD surface modulus, E_{LWD}, to any of the mechanical properties obtained from the hysteresis loops of the IC responses. Yet, some factors must be taken into consideration, for instance the ranges of nonlinear k parameters used for the IC are more limited to those for the LWD, as the former easily yield magnitudes of resilient modulus that fall outside the typical ranges seen for both base

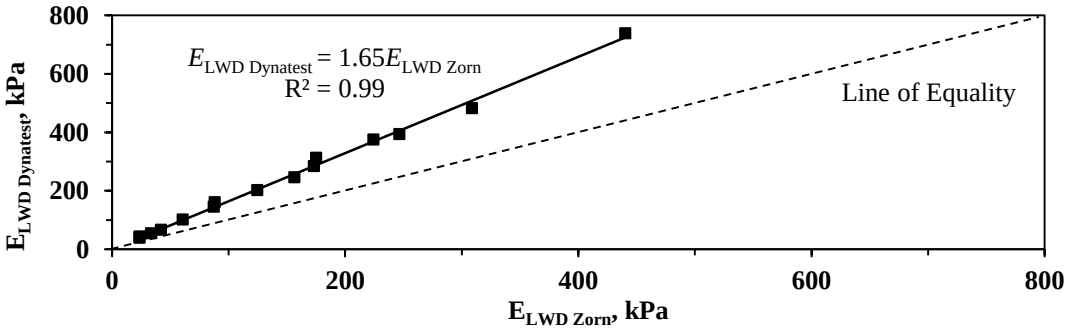

Figure 21 – Relationship of E_{LWD} for Zorn and Dynatest LWD for different soil properties.

and subgrade materials. This is because larger stresses may develop close to the surface, depending on the contact area, than those observed by regular traffic and typical in-situ testing, such as LWD. The MEPDG models were developed and calibrated to fit the latter conditions rather and may not be suitable for conditions resulting from roller compaction.

4. Summary and Conclusions

A parametric study was carried using 3-D finite element analysis to estimate the depth of influence based on the different type of responses, i.e. stress, strain and deflection, due to roller compaction and light weight deflectometer (LWD) testing. A single layered system consisting of subgrade was considered for the analysis, which made use of the nonlinear constitutive material model for unbound granular and subgrade materials as recommended by the MEPDG. Among the findings obtained from the analysis of IC stand out the following:

- Depth of influence in terms of stress and strain decreased slightly as subgrade became more rigid and more granular, whereas influence depth significantly increase as subgrade became more clayey (represented by nonlinear parameter k_3). Influence depth of 10% of the surface stress varied from about 1 m (40 in.) to 1.8 m (70 in.) from the pavement surface. Influence depth based on 10% of the surface deflection reached deeper to about 2 m (80 in.). If a similar criterion is established for strain responses, influence depths could reach to 2.5 m (100 in.) or more, but given the model's dimensions this could not be determined for some cases.
- Vertical compressive stresses decay slowly beyond the depth where a stress level of 10% of surface stress occurs. Thus, setting lower level levels of stress due to roller compaction may lead to have depths of influence to occur deeper than 2.5 m (100 in.) which happens to be the model's depth.
- Using hysteresis loops, secant and tangent stiffness and moduli were determined for all roller compaction cases considered. Little difference is observed in magnitudes of secant to tangent stiffness, and secant to tangent moduli, in most cases.
- Magnitudes of the nonlinear parameters may yield extremely high magnitudes of stiffness and modulus that may fall outside the typical ranges of a subgrade material. This problem is related the model that makes use of stress parameters, such as bulk stress, which can be large in magnitude due to the large stresses occurring underneath the roller at the soil surface at peak loads.

- Use of MEPDG representative modulus, as determined by the NCHRP 1-28A recommended state of stress values, does significantly underpredict the soil response when compared to the nonlinear response.

Two common LWDs, Zorn and Dynatest, were studied by means of finite element modeling for determining their depth of measurement influence. Similar to the analysis of IC to better address the soil response under loading, a modified version of the MEPDG constitutive model for geomaterials was considered. The applied impact loads and their duration were set to be equal in both LWD devices.

- Differences in responses between these devices occurred due to the mechanism of the plate contact with the soil surface. On average, the vertical stresses were 1.5-1.6 greater for the Zorn LWD than for the Dynatest LWD. Considering the dynamic nature of the load applied, the results showed propagation of stresses toward the outer boundaries of the plates, creating higher stress concentrations at the edge of the plate. Similarly, the Zorn LWD generated peak vertical strains 1.2-1.8 times greater than the Dynatest LWD, and surface deflections 1.4-1.7 times greater than those obtained under the Dynatest plate. The relationship between the surface moduli of the LWD devices corroborates the empirical evidence reported by several studies in the past.
- The influence depth based on the stress criterion was found to lie between 2.0-2.5 times the diameter of the LWD plate, decreasing as the geomaterial becomes stiffer and more granular. The depth of influence based on strain varied between 2.0 and 3.5 times the diameter of the plate while depth of influence based on deflection varied between 3 and 4 times the plate diameter, both decreasing as the geomaterial becomes less granular and more clayey. These depths of influence are greater than those reported in the literature because the dynamic nature of the load applied was considered. The influence depths of the Dynatest LWD appear to be more sensitive to the geomaterial nonlinear parameters than the Zorn LWD.

5. Future Work and Recommendations

At present moment, a larger database of LWD pavement responses and IC roller responses, for both single and two-layered systems (base and subgrade), is currently under development. This larger database will provide more rigorous results as to consider different combinations of pavements. The purpose of developing these databases is to relate LWD surface modulus, E_{LWD}, to any of the mechanical properties obtained from the hysteresis loops of the IC responses. Moreover, validation of model with field data is required to validate the FE model and to develop a relationship between the models to the field responses.

6. References

Alshibli, K. A., Abu-Farsakh, M., and Seyman, E. (2005). "Laboratory Evaluation of the Geogauge and Light Falling Weight Deflectometer as Construction Control Tools." *Journal of Materials in Civil Engineering*, ASCE, 17(5), 560–569.

Bilodeau, J.-P., and Doré, G. (2014). "Stress distribution experienced under a portable light-weight deflectometer loading plate." *International Journal of Pavement Engineering*, 15(6), 564–575.

Chiroux, R. C., Foster, W. A., Johnson, C. E., Shoop, S. A., and Raper, R. L. (2005). "Three-Dimensional Finite Element Analysis of Soil Interaction with a Rigid Wheel." *Applied Mathematics and Computation*, 162(2), 707–722.

Fleming, P. R., Frost, M. W., and Rogers, C. D. F. (2000). "A comparison of devices for measuring stiffness in situ." *Proceedings of the Unbound Aggregates in Road Construction—UNBAR 5*, CRC Press (Taylor & Francis Group), New York, NY, 193–200.

Hügel, H. M., Henke, S., and Kinzler, S. (2008). "High-Performance Abaqus Simulations in Soil Mechanics." *2008 ABAQUS Users' Conference*, Newport, RI, 1–15.

Khazanovich, L., Celauro, C., Chadbourn, B., Zollars, J., and Dai, S. (2006). "Evaluation of Subgrade Resilient Modulus Predictive Model for Use in Mechanistic-Empirical Pavement Design Guide." *Transportation Research Record: Journal of the Transportation Research Board*, National Research Council, Washington, D.C., 1947, 155–166.

Kim, K. (2010). "Numerical Simulation of Impact Rollers for Estimating the Influence Depth of Soil Compaction." Texas A&M University.

Mazari, M., Navarro, E., Abdallah, I., and Nazarian, S. (2014). "Comparison of numerical and experimental responses of pavement systems using various resilient modulus models." *Soils and Foundations*, 54(1), 36–44.

Mooney, M. A., and Facas, N. W. (2013). *Extraction of Layer Properties from Intelligent Compaction Data*. *Final Report for NCHRP Highway IDEA Project 145*, Washington, DC.

Mooney, M. A., and Miller, P. K. (2009). "Analysis of Lightweight Deflectometer Test Based on In Situ Stress and Strain Response." *Journal of Geotechnical and Geoenvironmental Engineering*, American Society of Civil Engineers, 135(2), 199–208.

Mooney, M. A., Rinehart, R. V., Facas, N. W., Musimbi, O. M., and White, D. J. (2010). *NCHRP Report 676: Intelligent Soil Compaction Systems*. Washington, DC, 165.

Nazzal, M., Abu-Farsakh, M., Alshibli, K., and Mohammad, L. (2004). "Evaluating the Potential Use of a Portable LFWD for Characterizing Pavement Layers and Subgrades." *Geotechnical Engineering for Transportation Projects, GeoTrans 2004, GSP 126, July 27-31, 2004*, M. K. Yegian and E. Kavazanjian, eds., American Society of Civil Engineers, Los Angeles, CA, 915–924.

Oh, J. H. (2011). *Comparison of Resilient Modulus Values Used in Pavement Design*. *Final Report BDL76-1*, College Station, TX.

Patrick, J., and Werkmeister, S. (2010). *Compaction of Thick Granular Layers, NZ Transport Agency Research Report No. 411*. New Zealand Transport Agency, Wellington, New Zealand, 40.

Rinehart, R. V., and Mooney, M. A. (2009). "Measurement depth of vibratory roller-measured soil stiffness." *Géotechnique*, 59(7), 609–619.

Siekmeier, J. A., Young, D., and Beberg, D. (2000). "Comparison of the Dynamic Cone Penetrometer with Other Tests During Subgrade and Granular Base Characterization in Minnesota." *Symposium on Nondestructive Testing of Pavements and Backcalculation of Moduli: Third Volume, ASTM STP 1375*, S. D. Tayabji and E. O. Lukanen, eds., American Society for Testing and Materials, Seattle, WA, 175–188.

Stamp, D. H., and Mooney, M. A. (2013). "Influence of Lightweight Deflectometer Characteristics on Deflection Measurement." *Geotechnical Testing Journal*, 36(2), 216–226.

Terzaghi, K., and Peck, R. B. (1967). *Soil mechanics in engineering practice*. Wiley, 729.

Velasquez, R., Hoegh, K., Yut, I., Funk, N., Cochram, G., Marasteanu, M., and Khazanovich, L. (2009). *Implementation of the MEPDG for New and Rehabilitated Pavement Structures for Design of Concrete and Asphalt Pavements in Minnesota. Research Report MN/RC 2009-06*. St. Paul, MN.

Vennapusa, P. K. R., and White, D. J. (2009). "Comparison of Light Weight Deflectometer Measurements for Pavement Foundation Materials." *Geotechnical Testing Journal*, 32(3), 239–251.

Wang, L., Zhang, B., Wang, D., and Yue, Z. (2007). "Fundamental Mechanics of Asphalt Compaction Through FEM and DEM Modeling." *Analysis of Asphalt Pavement Materials and Systems Analysis: Engineering Methods, GSP 176*, L. Wang and E. Masad, eds., American Society of Civil Engineers, Boulder, CO, 45–63.

White, D. J., Vennapusa, P. K. R., Zhang, J., Gieselman, H., and Morris, M. (2009). *Implementation of Intelligent Compaction Performance Based Specifications in Minnesota*. *MN/RC 2009-14*, Earthworks Engineering Research Center, Iowa State University, Ames, IA, 337.

Xia, K., and Pan, T. (2010). "Understanding Vibratory Asphalt Compaction by Numerical Simulation." *International Journal of Pavement Research and Technology*, 4(3), 185–194.